

Growth of Barium Chlorapatite Crystals from a Sodium Chloride Flux

Shuji Oishi,* Noriyuki Michiba,[†] Nobuo Ishizawa,^{††} Juan Carlos Rendon-Angeles,^{†††} and Kazumichi Yanagisawa^{†††}

Department of Environmental Science and Technology, Faculty of Engineering, Shinshu University, Wakasato, Nagano 380-8553

[†]Department of Chemistry and Material Engineering, Faculty of Engineering, Shinshu University, Wakasato, Nagano 380-8553

^{††}Materials and Structures Laboratory, Tokyo Institute of Technology, Nagatsuta, Midori-ku, Yokohama 226-8503

^{†††}Research Laboratory of Hydrothermal Chemistry, Faculty of Science, Kochi University, Akebono, Kochi 780-8520

(Received April 5, 1999)

Large and well-formed crystals of barium chlorapatite [$\text{Ba}_5\text{Cl}(\text{PO}_4)_3$] were grown for the first time from a sodium chloride flux. The solubility of $\text{Ba}_5\text{Cl}(\text{PO}_4)_3$ in NaCl increased with increasing temperature, reaching about 1.9 mol% solubility at 1100 °C. The crystal growth of $\text{Ba}_5\text{Cl}(\text{PO}_4)_3$ was conducted by heating a mixture of solute and flux at 1100 °C for 10 h, and then cooling to 500 °C at a rate of 5 °C h⁻¹. Colorless and transparent prismatic crystals with lengths of up to 12 mm and widths of 3 mm were grown from high-temperature solutions containing 0.4–2.2 mol% solute. The most suitable solute content for the growth of prismatic crystals was 1.2 mol%. The prismatic crystals were bounded by the {10 $\bar{1}$ 0} and {10 $\bar{1}$ 1} faces. The aspect ratios were in the region of 1.1 to 4.8. Needle crystals with lengths of up to 4 mm and widths of 60 μm were obtained during every growth run. The needle crystals were elongated in the (0001) directions, with aspect ratios ranging from 43 to 56. The major constituents were almost homogeneously distributed in the prismatic and needle crystals.

Apatites are well known for their applications as phosphatic fertilizers, fluorescent-lamp phosphors, laser hosts, and biocompatible materials.¹ The formula of apatite allows a wide variety of substitutions, which yield a vast number of phases with essentially identified structures.¹ Barium chlorapatite has the formula $\text{Ba}_5\text{Cl}(\text{PO}_4)_3$ [pentabarium chloride tris(phosphate)]. The crystals of $\text{Ba}_5\text{Cl}(\text{PO}_4)_3$ belong to the hexagonal system with space group $P6_3/m$.²

A crystalline powder of $\text{Ba}_5\text{Cl}(\text{PO}_4)_3$ has been synthesized by a solid state reaction method.^{3–5} $\text{Ba}_3(\text{PO}_4)_2$ in HCl has been completely converted to $\text{Ba}_5\text{Cl}(\text{PO}_4)_3$.⁶ Hexagonal $\text{Ba}_5\text{Cl}(\text{PO}_4)_3$ prisms with lengths of up to 0.3 mm have been prepared by the hydrothermal method.² Irregular-shaped crystals^{7,8} and uniform fibers⁹ of $\text{Ba}_5\text{Cl}(\text{PO}_4)_3$ have also been grown by the BaCl_2 flux method. No report on the growth of $\text{Ba}_5\text{Cl}(\text{PO}_4)_3$ crystals from a NaCl flux has been published. The solubility of $\text{Ba}_5\text{Cl}(\text{PO}_4)_3$ in NaCl has not yet been reported.

We have, for the first time, grown well-formed $\text{Ca}_5\text{Cl}(\text{PO}_4)_3$ crystals of up to 4 mm \times 1.2 mm in size from a NaCl flux.¹⁰ The obtained crystals were divided into two distinct morphological types: prisms and needles. Sodium chloride was found to be a suitable flux to grow these crystals.

In this work, NaCl was chosen as a flux to grow crystals of $\text{Ba}_5\text{Cl}(\text{PO}_4)_3$ on the basis of our experience in growing $\text{Ca}_5\text{Cl}(\text{PO}_4)_3$ crystals.¹⁰ Sodium chloride has a common an-

ion (Cl^-) with the solute. There is a difference in the cationic valency between the flux (1+) and the solute (2+). Another difference is established by the cationic radii between the flux (Na^+) and the solute (Ba^{2+}). In this way, there are a similarity and differences between NaCl and $\text{Ba}_5\text{Cl}(\text{PO}_4)_3$. Furthermore, NaCl has a low melting point with sufficient solubility in water and low toxicity to humans. Sodium chloride was expected to be a good flux.

The present paper describes the growth of $\text{Ba}_5\text{Cl}(\text{PO}_4)_3$ crystals from a NaCl flux. The effect of the solute content on crystal growth was studied. The morphology, density, and imperfections of the resulting crystals were examined. The solubility of $\text{Ba}_5\text{Cl}(\text{PO}_4)_3$ in NaCl was also measured.

Experimental

Solubility. The solubility of $\text{Ba}_5\text{Cl}(\text{PO}_4)_3$ in NaCl was determined by measuring the mass loss of $\text{Ba}_5\text{Cl}(\text{PO}_4)_3$ in NaCl melts at temperatures of between 700 and 1100 °C. Mixtures of excess crystals (1–5 mm, 0.5–2.0 g) of $\text{Ba}_5\text{Cl}(\text{PO}_4)_3$ and NaCl powder (about 4 g) were put into platinum vessels. After heating the mixture for 1 h at a preset temperature, undissolved crystals were present upon quenching. The undissolved crystals were separated from the solidified saturated solution in warm water and reweighed. The loss in mass due to dissolution represents the solubility at that temperature. The eutectic temperature of the $\text{Ba}_5\text{Cl}(\text{PO}_4)_3$ –NaCl system was determined on the basis of differential thermal analysis (DTA) curves.

Flux Growth. Reagent-grade $(\text{NH}_4)_2\text{HPO}_4$, BaCO_3 , $\text{BaCl}_2 \cdot 2\text{H}_2\text{O}$, and NaCl were used for the flux growth of $\text{Ba}_5\text{Cl}(\text{PO}_4)_3$ crystals. A mixture of $6(\text{NH}_4)_2\text{HPO}_4 + 9\text{BaCO}_3 + \text{BaCl}_2 \cdot 2\text{H}_2\text{O}$ powders was used as a solute. Sodium chloride powder was used as the flux. Mixtures containing solutes of 0.4 to 2.2 mol% were prepared in 0.1 mol% increments. The masses of the mixtures were in the region of 25.6–27.7 g (about 25 g as $\text{Ba}_5\text{Cl}(\text{PO}_4)_3\text{--NaCl}$). The mixtures were put into 30 cm^3 platinum crucibles. After closing the lids, the crucibles were placed in an electric furnace with silicon carbide heating elements. The crucibles were heated to 1100 °C at a rate of about 45 °C h^{-1} , held at this temperature for 10 h, and then cooled to 500 °C at a rate of 5 °C h^{-1} . When the cooling program was completed, the crucibles were allowed to cool down to room temperature. The crystalline products were then separated by dissolving the flux in warm water.

Characteristics. The obtained crystals were examined using an optical microscope and a scanning electron microscope (SEM). The crystal phases were identified by X-ray diffraction (XRD). The length, L (parallel to the $\langle 0001 \rangle$ directions), and width, W (perpendicular to the $\langle 0001 \rangle$ directions), of the $\text{Ba}_5\text{Cl}(\text{PO}_4)_3$ crystals grown were measured. Based on the aspect ratio (L/W) of the crystals, they were divided into two morphological types: prisms with $L/W \leq 10$ and needles which had $L/W > 10$. After each growth run, the average length (L_{av}) and width (W_{av}) of the first 30 largest crystals with prismatic or needle forms were calculated. The XRD data of the orientated crystals grown were obtained. The interfacial angles of the crystals were also measured. The density of the crystals was determined pycnometrically. A SEM equipped with an energy dispersive X-ray spectrometer (EDS) was used to study any variations in the concentration of the major constituents in the grown crystals. The presence of impurities from the NaCl flux and Pt crucible was also checked.

Results and Discussion

Solubility of $\text{Ba}_5\text{Cl}(\text{PO}_4)_3$ in NaCl . The dependence of the solubility on the temperature is shown in Fig. 1. A mixture of $\text{Ba}_5\text{Cl}(\text{PO}_4)_3\text{--NaCl}$ did not melt at 700 °C. At 800 °C, $\text{Ba}_5\text{Cl}(\text{PO}_4)_3$ was dissolved in NaCl at a concentration of about 0.3 mol% (about 5.7 g in 100 g NaCl). The solubility gradually increased with temperature, with $\text{Ba}_5\text{Cl}(\text{PO}_4)_3$ reaching a solubility of about 1.9 mol% (about 33.6 g in 100 g NaCl) at 1100 °C. The obtained solubility curve had an appreciable temperature coefficient of solubility. Therefore, $\text{Ba}_5\text{Cl}(\text{PO}_4)_3$ could be crystallized by slowly cooling the solutions. Thus, NaCl is expected to be a suitable flux for growing $\text{Ba}_5\text{Cl}(\text{PO}_4)_3$ crystals.

An endothermic peak appeared at 790 ± 5 °C on the DTA curve obtained during heating a mixture of $\text{Ba}_5\text{Cl}(\text{PO}_4)_3$ and NaCl powders. The peak was due to a eutectic reaction. It was found that the eutectic temperature of the $\text{Ba}_5\text{Cl}(\text{PO}_4)_3\text{--NaCl}$ system was 790 ± 5 °C. Judging from the solubility curve and eutectic temperature, the eutectic composition was considered to be about $\text{Ba}_5\text{Cl}(\text{PO}_4)_3$ (0.3 mol%)– NaCl (99.7 mol%).

Figure 1 shows that mixtures containing 0.4–1.9 mol% solute are unsaturated at a soak temperature of 1100 °C of the flux growth runs. Based on the solubility curve, the saturation temperatures of mixtures containing 0.5, 1.2, and 1.9 mol% solute are around 890, 1025, and 1100 °C, respectively. The

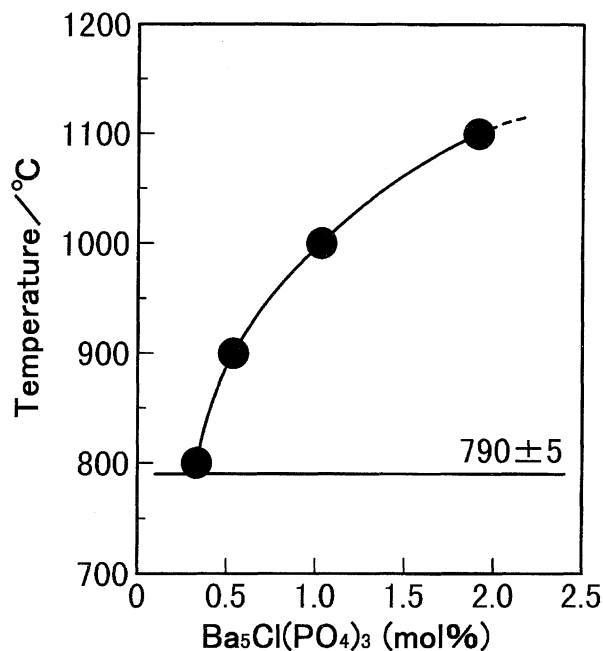


Fig. 1. Solubility of $\text{Ba}_5\text{Cl}(\text{PO}_4)_3$ in NaCl as a function of temperature.

solubility at 1100 °C corresponds to a starting composition of $\text{Ba}_5\text{Cl}(\text{PO}_4)_3$ (1.9 mol%)– NaCl (98.1 mol%). In the case of mixtures containing 2.0–2.2 mol% solute, the solution is incomplete at this soak temperature.

Preliminary experiments confirmed that maintaining a given temperature for 1 h was sufficient for equilibration. The evaporation of NaCl was less than 10 mass% during these solubility experiments. The evaporation had little influence on the solubility.

Flux Growth of $\text{Ba}_5\text{Cl}(\text{PO}_4)_3$ Crystals. Large and well-formed prism- and needle-shaped $\text{Ba}_5\text{Cl}(\text{PO}_4)_3$ crystals having lengths of up to 12 mm and widths of 3 mm were grown from the NaCl flux. The obtained crystals were colorless and transparent. The crystals tended to grow at the bottom of the crucible due to the difference between the densities of the solute and flux. Prismatic and needle crystals were grown from mixtures containing 0.4–2.2 mol% solute. When mixtures containing 0.4–1.8 and 1.9–2.2 mol% solute were used, long prismatic and short prismatic crystals were grown, respectively. At all growth runs, needle crystals were grown. Typical long and short prismatic crystals of $\text{Ba}_5\text{Cl}(\text{PO}_4)_3$ are shown in Figs. 2 and 3, respectively. Needle crystals of $\text{Ba}_5\text{Cl}(\text{PO}_4)_3$ are shown in Fig. 4.

The average length (L_{av}) and width (W_{av}) of the prismatic crystals are plotted against the solute content in Fig. 5. Large crystals with $L_{\text{av}} = 6.6$ mm were grown from a mixture containing 1.2 mol% solute. Any further increase in the solute content resulted in a decrease in the L_{av} value. A mixture containing 0.4 mol% solute resulted in crystals with $W_{\text{av}} = 0.8$ mm. The W_{av} value gradually increased with increasing solute content. Mixtures containing a solute of 1.9–2.2 mol% produced crystals with W_{av} values of 2.2–2.3 mm. There was no marked difference among the W_{av} values. The as-

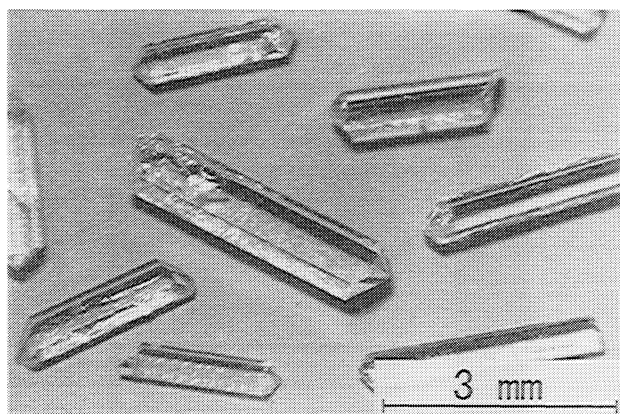


Fig. 2. Optical micrograph showing long prismatic crystals of $\text{Ba}_5\text{Cl}(\text{PO}_4)_3$ grown from NaCl flux.

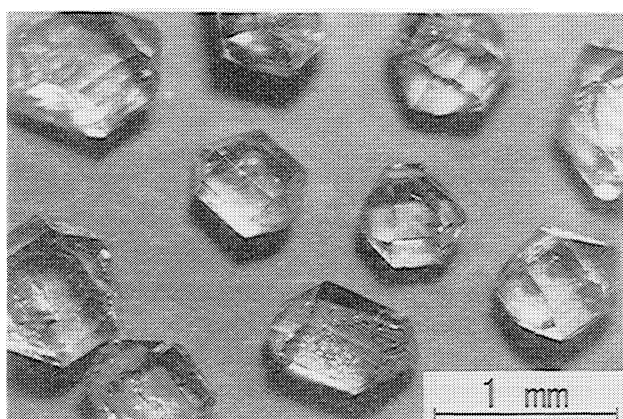


Fig. 3. Optical micrograph showing short prismatic crystals of $\text{Ba}_5\text{Cl}(\text{PO}_4)_3$ grown from NaCl flux.

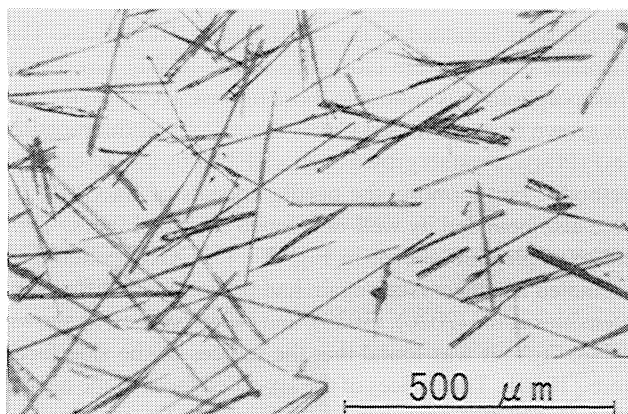


Fig. 4. Optical micrograph showing needle crystals of $\text{Ba}_5\text{Cl}(\text{PO}_4)_3$ grown from NaCl flux.

pect ratios ($L_{\text{av}}/W_{\text{av}}$) of the crystals were in the region of 1.1–4.8. The values decreased with increasing solute content. The forms of the prismatic crystals varied from long prismatic to short prismatic.

Needle crystals of $\text{Ba}_5\text{Cl}(\text{PO}_4)_3$ with dimensions of up to $L = 4$ mm and $W = 60$ μm were grown from mixtures containing solute of 0.4–2.2 mol%. The average length (L_{av}) and width (W_{av}) of the needle crystals are plotted against solute content in Fig. 6. A mixture containing a solute of

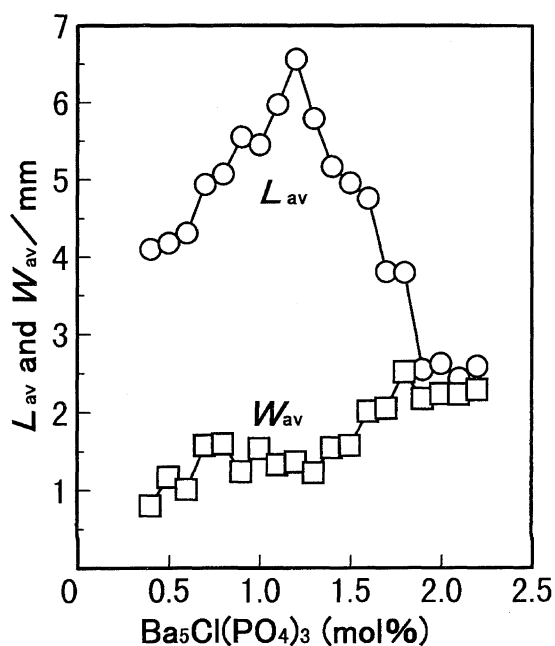


Fig. 5. Variation in average length, L_{av} , and width, W_{av} , of prismatic crystals of $\text{Ba}_5\text{Cl}(\text{PO}_4)_3$ with solute content.

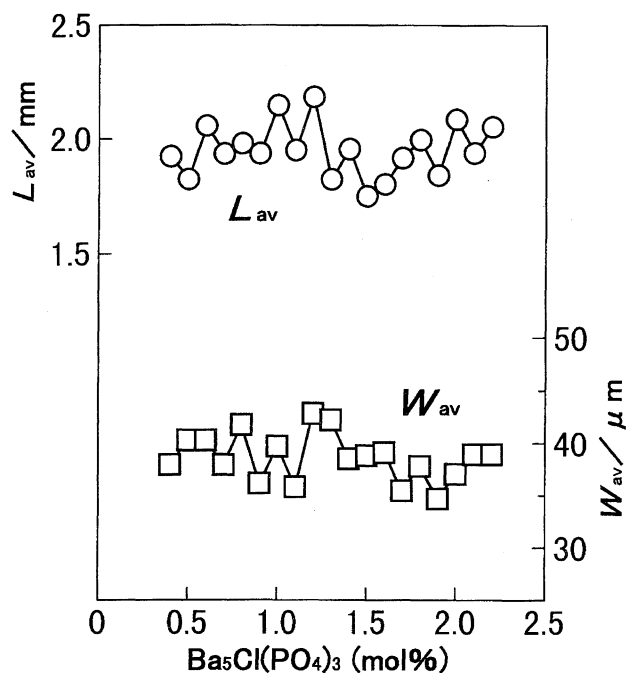


Fig. 6. Variation in average length, L_{av} , and width, W_{av} , of needle crystals of $\text{Ba}_5\text{Cl}(\text{PO}_4)_3$ with solute content.

0.4–2.2 mol% produced needle crystals with L_{av} values of 1.8–2.2 mm and W_{av} values of 35–43 μm . The aspect ratios of the crystals ranged from 43 to 56. These values were independent of the solute content.

A mixture containing 1.2 mol% solute produced 2.93 g crystals. About 68 mass% of the solute (4.33 g) employed was recovered in the form of prismatic and needle crystals. In a calculation using the starting composition and eutectic composition, the masses of $\text{Ba}_5\text{Cl}(\text{PO}_4)_3$ crystals grown and a powder contained in a eutectic mixture were 3.26 and 1.07

g, respectively. The mass of the obtained crystals was about 90% of the calculated value. The agreement between the observed and calculated mass of grown crystals was good.

During these growth runs, evaporation of the NaCl flux was less than 30 mass%. The evaporation had more or less influence on the growth of $\text{Ba}_5\text{Cl}(\text{PO}_4)_3$ crystals. In practice, a combination of slow cooling with evaporation of the flux produced crystals of $\text{Ba}_5\text{Cl}(\text{PO}_4)_3$. The platinum crucibles were found to be undamaged after use. The NaCl flux did not attack the crucibles. The resulting crystals could be readily separated from the flux in warm water because NaCl was easily soluble.

Characteristics of the $\text{Ba}_5\text{Cl}(\text{PO}_4)_3$ Crystals. The obtained prismatic and needle crystals were identified as $\text{Ba}_5\text{Cl}(\text{PO}_4)_3$ by their XRD patterns, shown in Figs. 7(a) and 7(d).¹¹

The prismatic crystals of $\text{Ba}_5\text{Cl}(\text{PO}_4)_3$ had a form of a hexagonal prism with pyramidal end faces. The surfaces of these crystals were very flat. A typical example is shown in Fig. 8. In order to determine the Miller indices of the crystal faces, orientated crystals were investigated by the

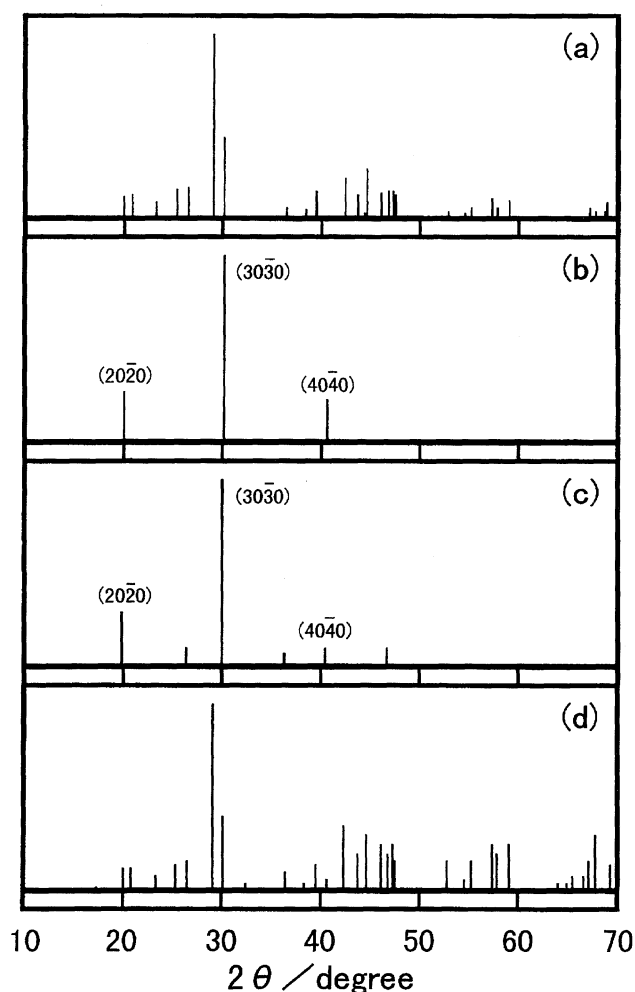


Fig. 7. XRD patterns ($\text{Cu K}\alpha$) of $\text{Ba}_5\text{Cl}(\text{PO}_4)_3$ crystals. (a): Pulverized crystallites of prismatic and needle crystals, (b): Orientated prismatic crystals, (c): Orientated needle crystals, and (d): JCPDS data.¹¹

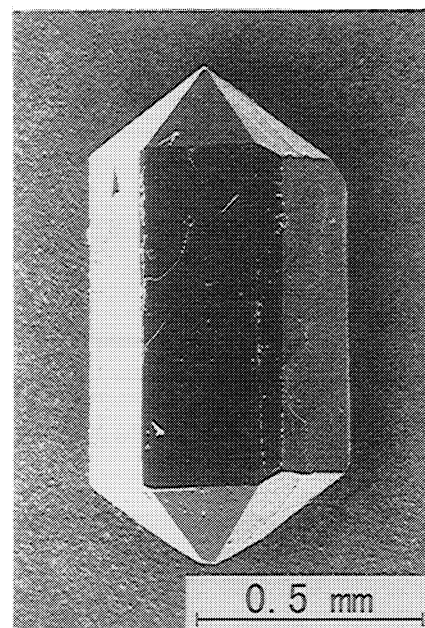


Fig. 8. SEM photograph showing a hexagonal prism with pyramidal end faces of $\text{Ba}_5\text{Cl}(\text{PO}_4)_3$.

XRD method. Figure 7(b) shows the XRD pattern of the orientated prismatic crystals. The diffraction intensities of the $(20\bar{2}0)$, $(30\bar{3}0)$, and $(40\bar{4}0)$ planes were predominant, indicating that the indices of the prismatic faces were $\{10\bar{1}0\}$. The interfacial angles between the prismatic and pyramidal faces were $49 \pm 1^\circ$. This value was in good agreement with the calculated interfacial angle of 49.3° between the $\{10\bar{1}0\}$ and $\{10\bar{1}1\}$ faces. On the basis of the XRD data and interfacial angle measurements, it was concluded that the prismatic crystals were bounded by the $\{10\bar{1}0\}$ and $\{10\bar{1}1\}$ faces. The prismatic crystals were elongated in the $\langle 0001 \rangle$ directions. This morphology is similar to those of the $\text{Ca}_5\text{Cl}(\text{PO}_4)_3$ crystals grown from NaCl and CaCl_2 fluxes^{10,12} and fluorapatite, $\text{Ca}_5\text{F}(\text{PO}_4)_3$, crystals grown from a KF flux by a slow-cooling method.¹³ Furthermore, the needle crystals of $\text{Ba}_5\text{Cl}(\text{PO}_4)_3$ were also bounded by well-developed six-sided faces. Typical examples are shown in Fig. 9. The XRD patterns of orientated needle crystals again had predominant diffraction intensities at the $(20\bar{2}0)$, $(30\bar{3}0)$, and $(40\bar{4}0)$ planes, as shown in Fig. 7(c). It was found that the indices of the side faces were $\{10\bar{1}0\}$. The indices of the six-sided faces of the needle crystals were the same as those of the prismatic crystals. The needle crystals were elongated in the $\langle 0001 \rangle$ directions.

Variations in the concentration of the major constituents in the grown $\text{Ba}_5\text{Cl}(\text{PO}_4)_3$ crystals were investigated by the EDS method. Figures 10(a) and 10(b) show a SEM photograph and EDS line profiles of the $\text{Ba}_5\text{Cl}(\text{PO}_4)_3$ crystal, respectively. Barium, phosphorus, and chlorine atoms were distributed almost homogeneously. According to the results, it was considered that oxygen atoms were also distributed almost homogeneously. Sodium from the NaCl flux was not detected. The chief disadvantage of the flux-growth technique is the incorporation of ions from the flux into the lattice of crystals. However, no Na^+ ions were incorporated

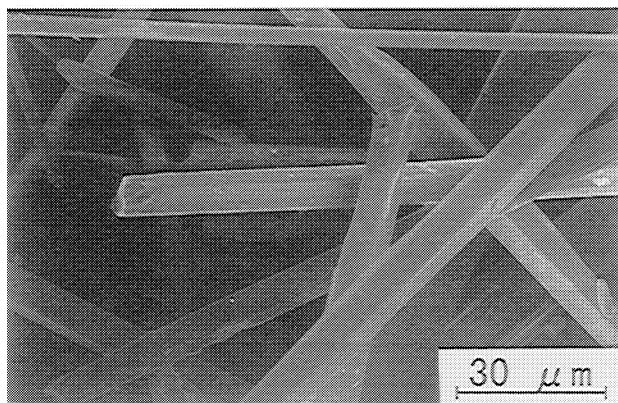


Fig. 9. SEM photograph showing six-sided needles of $\text{Ba}_5\text{Cl}(\text{PO}_4)_3$ crystals.

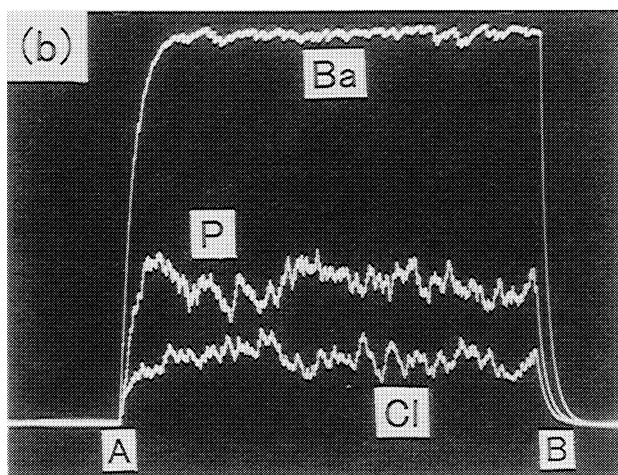
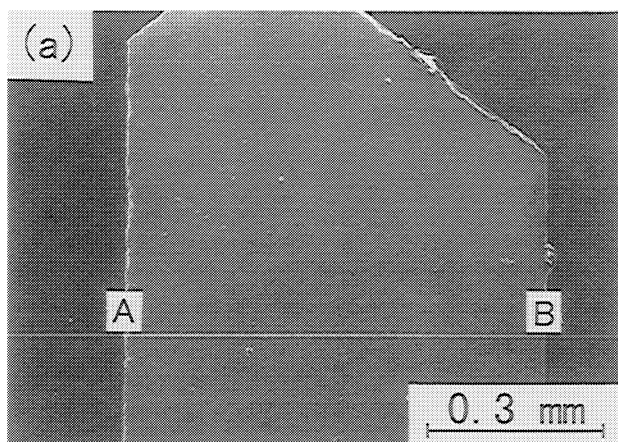


Fig. 10. SEM photograph (a) showing cross sectional interface of $\text{Ba}_5\text{Cl}(\text{PO}_4)_3$ crystal and EDS line profiles (b) of Ba, P, and Cl analyzed along the line between A and B.

into the crystals obtained in this work. This can be ascribed to the differences in the cationic valency and the radii between Na^+ and Ba^{2+} . Flux inclusions were rarely found in the crystals. Impurity incorporation of Pt from the crucible material was not detected in the crystals.

Based on the powder XRD data, the lattice parameters of the $\text{Ba}_5\text{Cl}(\text{PO}_4)_3$ crystals were $a = 10.27 \pm 0.01 \text{ \AA}$ and $c = 7.65 \pm 0.01 \text{ \AA}$. These values agree well with those ($a = 10.26 \text{ \AA}$ and $c = 7.65 \text{ \AA}$,¹ $a = 10.284 \text{ \AA}$ and $c = 7.651 \text{ \AA}$,² $a = 10.29 \text{ \AA}$ and $c = 7.65 \text{ \AA}$,⁸ $a = 10.26 \text{ \AA}$ and $c = 7.64 \text{ \AA}$ ¹¹) from the literature. The density was pycnometrically determined to be $4.80 \pm 0.01 \text{ g cm}^{-3}$. This was in good agreement with the calculated (4.80 g cm^{-3}) and literature (4.77^2 and $4.80^{11} \text{ g cm}^{-3}$) values. The observed lattice parameters and density were independent of the crystal forms.

Conclusions

Barium chlorapatite, $\text{Ba}_5\text{Cl}(\text{PO}_4)_3$, crystals were grown from a NaCl flux for the first time. Colorless and transparent $\text{Ba}_5\text{Cl}(\text{PO}_4)_3$ crystals with lengths of up to 12 mm and widths of 3 mm were obtained from high-temperature solutions containing a solute of 0.4–2.2 mol%. The resulting crystals were of two morphological types: prism and needle. The crystal sizes of prismatic crystals were dependent on the solute content. The solubility of $\text{Ba}_5\text{Cl}(\text{PO}_4)_3$ in NaCl increased with increasing temperature. Sodium chloride was found to be a suitable flux to grow these crystals.

This work was supported by a Grant-in-Aid for Scientific Research (C) No. 10650823 from the Ministry of Education, Science, Sports and Culture. A part of this work was carried out under the Collaborative Research Project of the Materials and Structures Laboratory, Tokyo Institute of Technology.

References

- 1 D. M. Roy, L. E. Drafall, and R. Roy, "Phase Diagrams: Materials Science and Technology," ed by A. M. Alper, Academic Press, New York (1978), Vol. V, pp. 185–239.
- 2 M. Hata, F. Marumo, S. Iwai, and H. Aoki, *Acta Crystallogr., Sect. B*, **B35**, 2382 (1979).
- 3 W. E. Klee and G. Engel, *J. Inorg. Nucl. Chem.*, **32**, 1837 (1970).
- 4 M. Kottaisamy, R. Jagannathan, P. Jeyagopal, R. P. Rao, and R. L. Narayanan, *J. Phys. D: Appl. Phys.*, **27**, 2210 (1994).
- 5 M. Sato, T. Tanaka, and M. Ohta, *J. Electrochem. Soc.*, **141**, 1851 (1994).
- 6 A. H. Hoekstra, W. L. Wanmaker, and J. G. Verriet, *J. Inorg. Nucl. Chem.*, **32**, 2445 (1970).
- 7 L. H. Brixner and K. Babcock, *Mater. Res. Bull.*, **3**, 817 (1968).
- 8 L. H. Brixner and J. F. Weiher, *J. Solid State Chem.*, **2**, 55 (1970).
- 9 K. Forster, M. Greenblatt, and J. H. Pifer, *J. Solid State Chem.*, **30**, 121 (1979).
- 10 S. Oishi and I. Sugiura, *Bull. Chem. Soc. Jpn.*, **70**, 2483 (1997).
- 11 JCPDS card 16-686.
- 12 S. Oishi and T. Kamiya, *Nippon Kagaku Kaishi*, **1993**, 1129.
- 13 S. Oishi and T. Kamiya, *Nippon Kagaku Kaishi*, **1994**, 800.